LANGMUIR

Article

pubs.acs.org/Langmuir

Stable and Functionalizable Quantum Dots with a Thin Zwitterionic Carboxybetaine Layer

Wei Yang, Jean-Rene Ella-Menye, Tao Bai, Andrew Sinclair, and Shaoyi Jiang*

Department of Chemical Engineering, University of Washington, Seattle, Washington 98195, United States

ABSTRACT: A new type of ligand chemistry, with a zwitterionic carboxybetaine headgroup and a bidentate thiol end group (CBSS), is introduced to promote the stability of quantum dots (QDs) with targeting capability. Results show that QDs are stable over a broad range of pH values after surface modification. Surface binding assays and cellular internalization studies show that QDs capped with CBSS exhibit low nonspecific adsorption. The CBSS ligand also allows the conjugation of highly specific targeting ligands while effectively maintaining the nonfouling background. This QD chemistry offers a unique approach to presenting abundant functional groups for ligand immobilization in a thin layer with an ultralow background and holds significant potential for imaging applications.

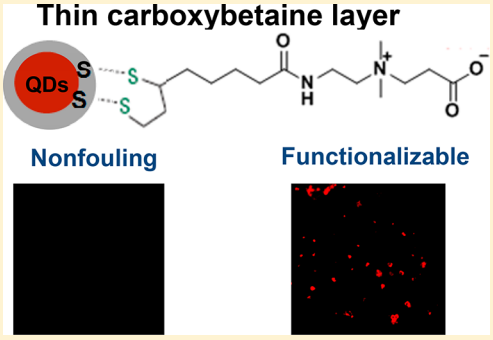

INTRODUCTION

Semiconductor nanocrystal quantum dots (QDs) are powerful photostable nanoemitters with uniquely narrow and tunable emission ranging from visible to infrared frequencies.[1−3] Luminescent QDs, such as CdSe-ZnS core−shell nanocrystals, in particular, have become one of the dominant classes of imaging probes as well as universal platforms for engineering multifunctional nanodevices.[4−6] Ideally, QDs should be easy to modify so that various secondary reporters or biomolecules can be appended for sensing and/or targeting cellular receptors.[7] QDs must maintain low nonspecific binding to proteins and cells, a small size, high quantum yield, and high stability over a wide pH range.[7] Careful engineering of QD probes is becoming increasingly important for the successful transition of this technology from proof-of-concept studies to real applications.[5]

For QDs to be useful as probes for the examination of biological specimens, their surfaces must be hydrophilic. Several strategies have been used to stabilize core−shell nanocrystals in aqueous solutions.[8,9] PEGylation has been shown to be compatible with QD surface chemistry[10] and has played a prevalent role in optimizing the *in vivo* pharmacokinetics of QD probes.[11] However, poly(ethylene glycol) (PEG) QDs tend to aggregate in high-salinity buffers. In addition, the PEG polymer substantially increases the size of QDs (>20 nm[7,12,13]), which decrease the QD sensitivity and may further limit intracellular mobility.[5,13,14] Recently, zwitterionic materials such as sulfobetaine[14−19] and phosphorylcholine[20] have been coated onto QDs to reduce the nonspecific interaction with cells.[1,14−20] The coated QDs exhibit much smaller diameters, weak nonspecific interactions with proteins, and strong resistance to pH and salinity.

QDs have been used in biotechnological applications that conventionally employ fluorescence over the past several years.[21] However, most ligands, including zwitterionic sulfobetaine and phosphorylcholine headgroups, lack accessible terminal functionalities. A recent study in which a click agent was introduced into the sulfobetaine headgroup for surface functionalization is interesting.[22] To introduce functional groups for subsequent coupling to target biomolecules, PEG derivatives with a variety of functional end groups such as biotin, amino, and carboxyl groups have been developed. A functional PEG derivative always needs to be mixed with nonfouling ligands (e.g., hydroxyl-terminated PEG) to create functional ability with a nonfouling background. Even for QDs capped with zwitterionic sulfobetaine[14−18] or phosphorylcholine ligands,[20] functional PEG ligands are introduced for subsequent coupling to target biomolecules. However, mixed nonfouling and functionalizable ligands or nonfouling ligands with additional functional groups will always be a compromise between nonfouling and functionalizable properties. Unreacted functional groups after surface functionalization can still be vulnerable to nonspecific protein adsorption, particularly from complex media.

Dihydrolipoic acid (DHLA) has been widely used as a surface ligand for cap exchange to prepare water-soluble QDs.[23] In this work, we used lipoic acid (LA) to modify QDs as a control system because it is both the starting material for our ligand with a zwitterionic carboxybetaine headgroup (CBSS) and has properties similar to those of DHLA. This CBSS surface platform presents an abundance of functional groups, enabling the creation of a wide range of functional nanoparticles while maintaining their ultralow fouling background for high QD stability and efficiency. The carboxybetaine headgroup itself intrinsically not only is nonfouling but also can be conveniently and effectively conjugated with molecular

Special Issue: Surfaces and Interfaces for Molecular Monitoring

Received: March 22, 2017
Revised: June 23, 2017
Published: June 24, 2017

DOI: 10.1021/acs.langmuir.7b00981
Langmuir 2017, 33, 8784−8789

Scheme 1. Synthesis Scheme of CBSS

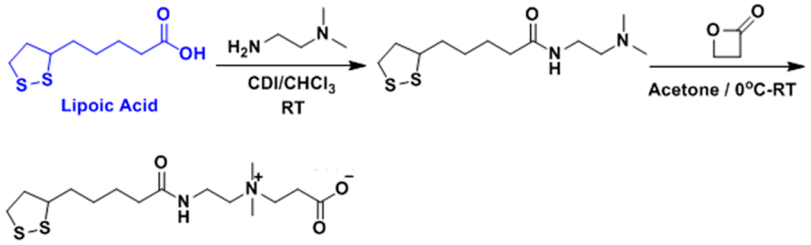

recognition elements via simple *N*-hydroxysuccinimide and 1-ethyl-3-(3- dimethylamino-propyl)-carbodiimide (NHS/EDC) chemistry under mild conditions. In one previous study, a carboxybetaine random polymer followed by postmodification was utilized to reduce nonspecific adsorption for QDs, but without demonstrating its functionalizable properties.[19] Here, we present a simple ligand (CBSS) that possesses nonfouling and functionalizable properties in one material for QDs.

EXPERIMENTAL SECTION

Materials. Lipoic acid, *N*,*N*-dimethylethylenediamine, 1-hydrobenzotriazole hydrate, 1-ethyl-3-(3-(dimethylamino)propyl)carbodiimide hydrochloride, *β*-propiolactone, and diisopropylethylamine were purchased from TCI America (Portland, OR). Controlled pore glass beads were purchased from Millipore Corp (Billerica, MA). TOPO-QDs (Qdot 605 organic quantum dots, CdSe/ZnS) were purchased from Life Technologies (Carlsbad, CA).

Synthesis of CBSS. As shown in Scheme 1, CBSS was synthesized in two steps starting with lipoic acid.

***N*-(2-Dimethylamino)ethyl)-5-(1,2-dithiolan-3-yl)pentanamide (1).** Lipoic acid (5.20 g, 25.2 mmol) and *N*,*N*-dimethylethylenediamine (3.03 mL, 27.7 mmol) were dissolved in dichloromethane (50.0 mL), and the solution was cooled to 0 °C. After stirring for 5 min, 1-hydrobenzotriazole hydrate (5.80 g, 37.9 mmol), 1-ethyl-3-(3-(dimethylamino)propyl)carbodiimide hydrochloride (7.25 g, 37.8 mmol), and diisopropylethylamine (26.3 mL, 151 mmol) were successively added to the solution. The mixture was allowed to warm to room temperature overnight and was stirred for 48 h. The solution was diluted with dichloromethane and extracted with water (3 × 20 mL) and brine (1 × 20 mL). The organic phase was dried over sodium sulfate, and the solvent was removed on a rotovap. The crude residue (yellow oil) was clean enough to be used in the next step without further purification. ^{1}H NMR (300 MHz, $CDCl_3$) δ (ppm): 6.10 (bs, 1H), 3.54 (m, 1H), 3.28 (dt, 2H, J = 11.4 Hz, 5.5 Hz), 3.12 (m, 2H), 2.42 (m, 1H), 2.37 (t, 2H, J = 5.9 Hz), 2.19 (s, 6H), 2.16 (t, 2H, J = 7.5 Hz), 1.89 (m, 1H), 1.65 (m, 4H), 1.44 (m, 2H).

3-((2-(5-(1,2-Dithiolan-3-yl)pentanamido)ethyldimethylammonio)propanoate (2) (CBSS). Compound **1** (6.97 g, 25.2 mmol) was dissolved in anhydrous tetrahydrofuran (50.0 mL), and the solution was cooled to 0 °C. *β*-Propiolactone (1.66 mL, 26.4 mmol) was added dropwise, and the solution was stirred and warmed to room temperature overnight. The mixture became a yellow suspension, and the yellow precipitate was filtered with a Buchner funnel, washed with acetone (3 × 50 mL), and dried under high vacuum. The pure product is obtained as a yellow powder (3.68 g, 10.58 mmol). Yield: 42%. ^{1}H NMR (300 MHz, D_2O) δ (ppm): 3.60 (t, 2H, J = 6.7 Hz), 3.53 (t, 2H, J = 5.9 Hz), 3.47 (t, 2H, J = 7.9 Hz), 3.31 (t, 2H, J = 6.4 Hz), 2.99 (s, 6H), 2.78 (m, 1H), 2.55 (t, 2H, J = 7.6 Hz), 2.34 (m, 1H), 2.14 (t, 2H, J = 7.1 Hz), 1.48 (m, 4H), 1.28 (m, 2H).

Synthesis of CBSS-QDs. CBSS-QDs were synthesized following a previously reported method.[1] One milliliter of a 75/25 methanol/isopropanol mixture was added to TOPO-QDs (250 pmol, 250 μL of 1 μM) to precipitate TOPO-QDs. They were mixed well and placed in a sealable centrifuge tube, sealed, and centrifuged for 3−5 min at 3000 rpm. The supernatant was discarded, and the pellet was redispersed in chloroform (1 mL). Ligands/QDs (10^5:1) were dissolved in water (1 mL). Sodium borohydride/ligands (2:1) were added to the solution and vigorously stirred for 20 min under N_2 gas flow at room temperature. The QD solution was added to the ligand solution and then intensely vortex mixed for 30 min at room temperature. The QDs were transferred from the organic layer to the aqueous layer. To remove excess free ligands, the QD solution was dialyzed using Amicon 50 kDa MW cutoff centrifugal filters.

Synthesis of LA-QDs. We then prepared the LA-QDs.[20] After methanol/isopropanol precipitation, the TOPO-QDs were redissolved in *n*-hexane (100 pmol). LA solution (800 nmol, 8 μL of 100 mM/ethanol), $NaBH_4$ (1 μL, 12 wt % in 14 N NaOH), and H_2O (31 μL) were added to the QD solution. Then the mixture was intensely vortex mixed for 30 min at room temperature. The *n*-hexane layer containing TOPO was removed, and the LA-QDs were collected with a filter and redispersed in PBS.

Imaging of the Intracellular Localization of QDs on Cells by TEM. TEM was applied to test the intracellular location of QDs in cells.[1] COS-7 cells were cocultured with the LA-QDs or CBSS-QDs for 24 h. To investigate the location of QDs in the COS-7 cells, the cells were treated for TEM observation. The cells were fixed with 2.5% glutaraldehyde in 0.1 M, pH 7.2 cacodylate buffer for 24 h at 4 °C and rinsed with cold 0.1 M, pH 7.2 cacodylate buffer three times. The cells were then fixed with 1% osmium tetraoxide for 1 h at 4 °C and washed with cold distilled water three times. The cells were dehydrated through a series of graded ethanol (50, 60, 70, 80, 90, 95, 98, and 100%) and propylene oxide solutions and finally embedded with epoxy resin (Epon 812). The samples were then polymerized at 60 °C for 24 h, cut into thin slices using an ultramicrotome, and collected on 200-mesh copper grids. The thin sections were stained with uranyl acetate (2% in ethanol) for 10 min and lead citrate for 5 min and observed on a TEM (JEOL 1320).

Nonspecific Protein Adsorption with QDs. Glass beads (100 μm diameter) were used to observe the nonspecific adsorption of QDs.[1] Beads were dispersed in PBS buffer. BSA was added to the solution (final concentration of 1 mg/mL), which was stirred overnight and dialyzed twice using Amicon 100 kDa MW cutoff centrifugal filters to remove the excess BSA. The beads in the solution were mixed with CBSS-QDs or LA-QDs in PBS buffer for 2 h. The ratio of QDs to beads was 10^7:1. The mixed solution was washed with PBS buffer and DI water three times each to remove excess QDs.

Cytotoxicity Assays of CBSS-QDs on Cells. To determine the cytotoxicity of CBSS-QDs, HeLa and COS-7 cells were tested by the MTT method using a Vybrant MTT cell proliferation assay kit.[24,25] Cells were seeded in 96-well cell culture plates in 100 μL of medium with 10% FBS serum under 5% CO_2 at 37 °C to allow 80−90% confluence. On the day of the test, cells were washed with PBS and incubated with 200 mL of fresh medium containing CBSS-QDs at various concentrations (10, 30, and 100 nM). After 24 h, cells were washed with PBS and incubated with 100 mL of medium and 50 mL of 12 mM MTT stock solution for 4 h at 37 °C. Then, the medium was removed, and 150 mL of DMSO was added and incubated for 10 min. The absorbance at 570 nm was measured using a plate reader.

QD Functionalization. To demonstrate easy conjugation of the QDs with CBSS ligands to biomolecular recognition elements,[1,14] CBSS-QDs were first activated with 10^4:1 NHS/EDC in water (100 mM, pH 5.5) for 30 min. Excess coupling reagent was removed twice by ultrafiltration through a 50 kDa cutoff filter. Activated QDs were then mixed with streptavidin (SA, 50 times) in sodium bicarbonate buffer (200 mM, pH 8.1) and incubated for 1 h. The SA-QDs were

DOI: 10.1021/acs.langmuir.7b00981
Langmuir 2017, 33, 8784−8789

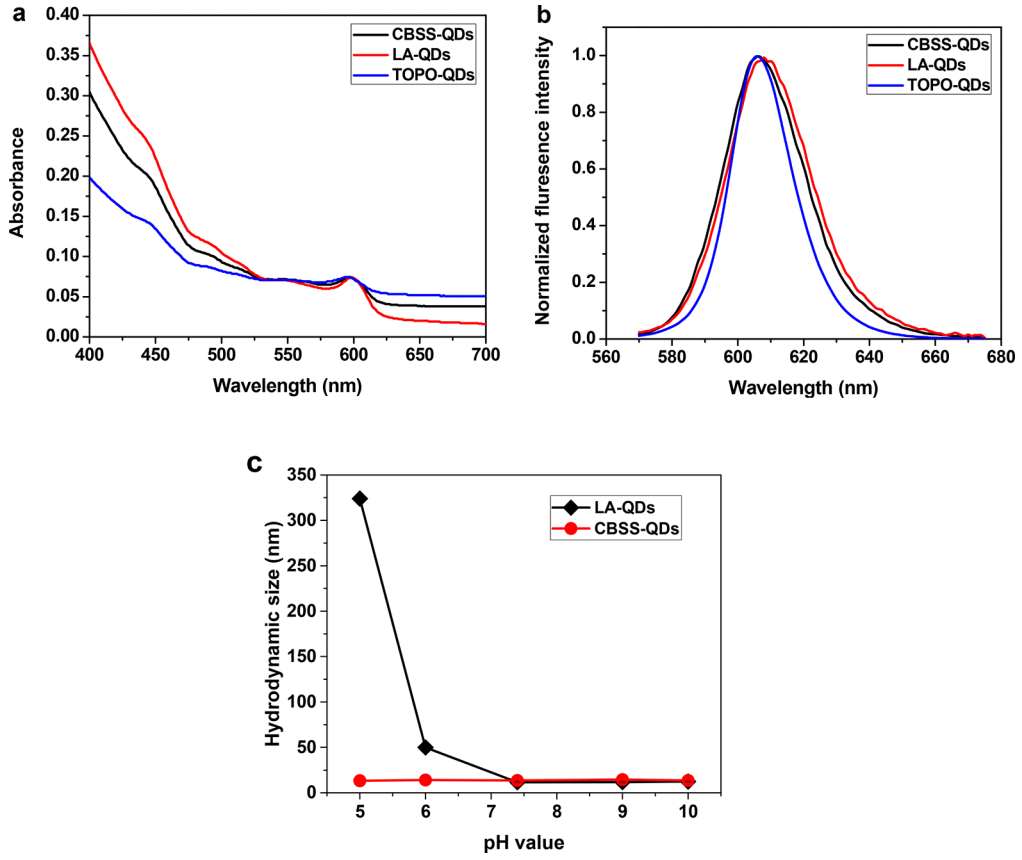

Figure 1. Characterization of CBSS- and LA- QDs: (a) Absorbance spectra of CBSS- and LA-QDs in PBS and TOPO-QDs in chloroform. (b) Fluorescence spectrum of CBSS- and LA-QDs in PBS and TOPO-QDs in chloroform. Fluorescence was measured at an excitation of 450 nm. (c) Hydrodynamic sizes of LA- and CBSS-QDs over the pH range from 5 to 10.

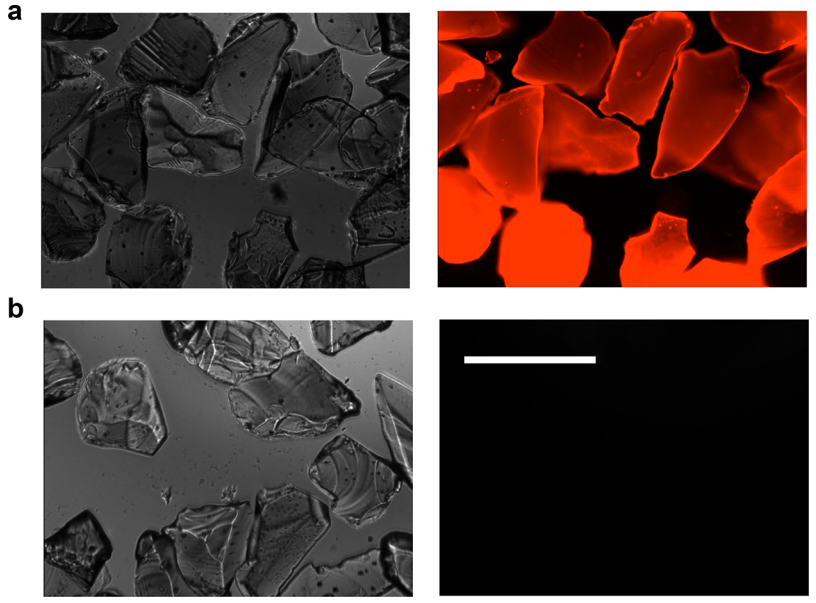

Figure 2. Nonspecific adsorption of (a) LA- and (b) CBSS-QDs on BSA-coated glass beads. Typical images of LA-QDs and CBSS-QDs under a bright field (left) and fluorescence (right), respectively (magnification, 20×; scale bar, 100 μm).

concentrated by ultrafiltration through a 50 kDa cutoff filter. The conjugation efficiency was checked by mixing 6 pmol of SA-QDs with biotin or SA-labeled silicon particles (1 μm diameter) over 15 min. The particles were washed three times in PBS by centrifugation and were photographed at 20× magnification on a Nikon Eclipse TE2000-U microscope.

RESULTS AND DISCUSSION

Characterization. After ligand exchange with LA or CBSS, the absorption and emission profiles of the CdSe/ZnS QDs changed slightly (Figure 1a). The emission was centered at 605 nm both before and after CBSS or LA ligand exchange (Figure

DOI: 10.1021/acs.langmuir.7b00981
Langmuir 2017, 33, 8784−8789

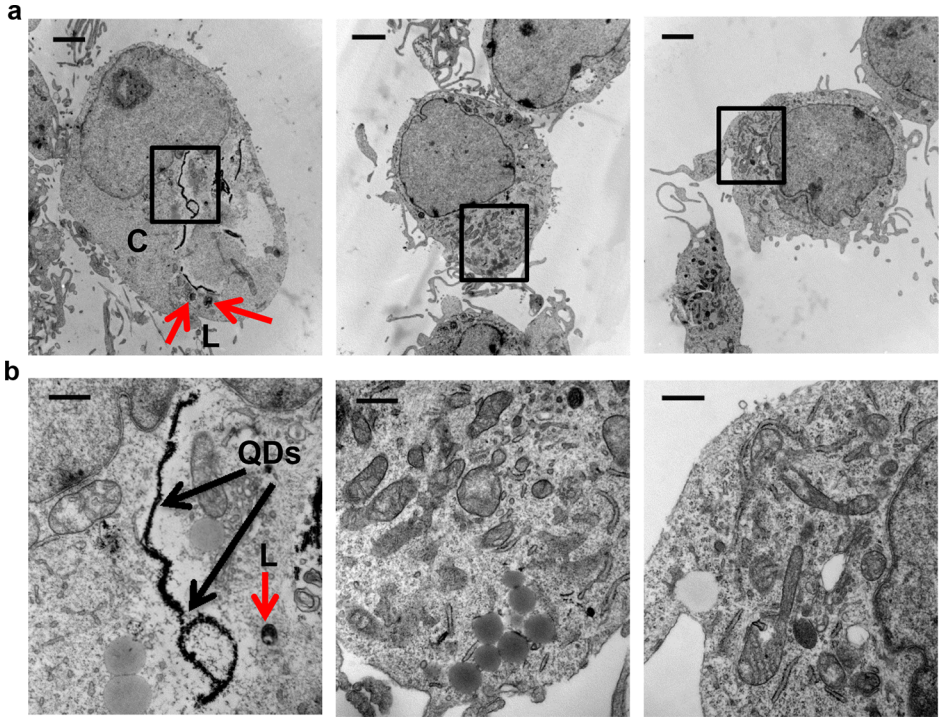

Figure 3. Intracellular localization of LA- (left) and CBSS-QDs (middle) in COS-7 cells and in COS-7 cells without QDs (right) under a magnification of (a) 8000×, scale bar 2 μm. (b) Enlarged image of the selected area at 40 000×, scale bar 500 nm. Black arrows indicate QDs. Red arrows indicate lysosome (L) and cytoplasm (C).

1b). The hydrodynamic diameter of CBSS-QDs was around 13.5 nm, a small increase from the original QD diameter of around 10 nm, indicating that the CBSS surface coating was about 1.8 nm thick. Usually, a polymeric shell produces relatively large hydrodynamic diameters on the order of 20−30 nm for an inorganic core/shell diameter of only 4−6 nm.[26] Thus, this thin CBSS coating on QDs presents a crucial advantage by maintaining their sensitivity for imaging, labeling, and sensing. We then tested the particle stability at different pH values. Figure 1c shows the hydrodynamic size of LA-QDs and CBSS-QDs at various pH values. It is evident that LA-QDs lose their colloidal stability and tend to slowly aggregate under acidic conditions but are easily dispersed in basic buffer solutions. Similar results have been shown in previous studies.[1,4] By contrast, QDs with a CBSS coating maintain excellent stability over pH values ranging from 5.0 to 10.0.

It should be pointed out that many current ligand-exchange approaches face a trade-off among size, stability, and derivatizability.[7] For example, in previous studies exploring the effect of PEG length on the *in vivo* behavior of QDs, the PEG length had to be increased to reduce nanoparticle uptake by the liver, even though this also increased the hydrodynamic diameter.[12] Thus, we expect that because the thin CBSS coating can offer increased stability without sacrificing the size and functionality of QDs, it holds tremendous potential for biomedical applications.

Nonspecific Adsorption on Beads. Nonspecific protein adsorption onto CBSS- or LA-QDs was investigated using bead adsorption assays (Figure 2). BSA and glass beads (diameter ∼100 μm) were incubated with CBSS- or LA-QDs. BSA was chosen because of its common use in ELISA and immunoblotting.[1] Under identical exposure time and excitation conditions, a large number of LA-QDs adsorbed on BSA (Figure 2). In contrast, after 2 h of contact with BSA and a wash with buffer/water, no detectable fluorescence signal was found for beads incubated with CBSS-QDs, indicating that the CBSS-QDs exhibit very low protein adsorption and do not have any apparent interactions with proteins such as entrapment or sequestration. Similar results have been reported previously for zwitterionic-sulfobetaine-coated QDs.[1] Our results confirm that zwitterionic carboxybetaine can greatly reduce nonspecific protein adsorption.

Intracellular Distribution of QDs. The intracellular distribution of CBSS- or LA-QDs after 24 h of incubation with COS-7 cells was investigated using TEM. As shown in Figure 3, most LA-QDs were found in the cytoplasm of COS-7 cells, which is indicative of lysosomal localization.[1] Some of the localized QDs were also found in lysosomes. The majority of LA-QDs found in cells appeared as aggregates; this phenomenon could be due to the fact that the LA shell coating does not offer sufficient stability for QDs, making them more susceptible to enzymatic digestion. Although most LA-QDs were found in aggregates, individual LA-QDs were also found in lysosomes and cytoplasm. However, no uptake was observed in the nuclei, indicating that LA-QDs are unable in penetrating cell nuclei.[27] Conversely, whereas both endosomes and lysosomes were observed in the TEM images, no CBSS-QDs were located within them. The significant differences in cellular uptake and distribution of LA- and CBSS-QDs indicate that the zwitterionic carboxybetaine QD surface enables QDs to avoid cell uptake.

Cytotoxicity of CBSS-QDs. We then examined the cytotoxicity of CBSS-QDs as a function of several factors, including concentration, size, and the presence of functional surface groups that could lead to cell death.[28] The cytotoxic effects of CBSS-QDs on HeLa and COS-7 cells were evaluated with MTT assays. Three different CBSS-QD concentrations (10, 50, and 100 nM) were assayed. As shown Figure 4, no

DOI: 10.1021/acs.langmuir.7b00981
Langmuir 2017, 33, 8784−8789

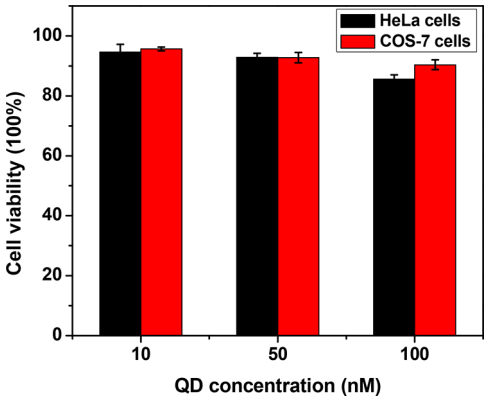

Figure 4. Cytotoxicity of CBSS-QDs to HeLa and COS-7 cells by MTT assay (n = 3).

significant decrease in cell viability was observed when CBSS-QDs were incubated with HeLa or COS-7 cells at the tested concentrations of up to 100 nM, confirming that CBSS-QDs have low cytotoxicity. This cytotoxicity evaluation coupled with the nonspecific bead adsorption tests and TEM images indicates that CBSS is capable of significantly reducing the cellular uptake and distribution of QDs and is a great probe for further bioimaging.

Functionalization of CBSS-QDs. In addition to enhancing the QD stability in different environments, the carboxybetaine end group also provides abundant functional groups for ligand immobilization. We next functionalized CBSS-QDs with biomolecules and demonstrated the absence of nonspecific adhesion *in vitro* after biomolecule immobilization. SA was immobilized onto CBSS-QDs via NHS/EDC, resulting in a high quantum yield and stable QDs.[14] We then tested the specific interactions of SA-conjugated QDs with biotinylated silicon particles. Figure 5a shows the high specificity of SA-QDs for biotinylated silicon particles. We also noticed that the SA-labeled CBSS-QDs did not bind SA-labeled silicon particles, again indicating ultralow nonspecific protein adsorption after functionalization (Figure 5b). This one-step functionalization process greatly simplifies conjugation to biomolecules with adjustable surface densities while ensuring that the post-functionalized surfaces possess excellent nonfouling properties.

CONCLUSIONS

We have demonstrated a functionalizable and stable surface platform for QDs that preserves QD optical properties, produces excellent nanoparticle stability, and maintains a small particle size. The absence of nonspecific protein and cell adsorption demonstrates the excellent nonfouling properties of the thin zwitterionic carboxybetaine coating. When SA was immobilized onto CBSS-QDs via NHS/EDC, SA-conjugated QDs were shown to specifically bind biotin-labeled silicon particles but not SA-labeled silicone particles. The unique properties of CBSS (i.e., ultralow fouling and functionalization potential) make this zwitterionic carboxybetaine polymer attractive as a next-generation QD coating for many biological imaging applications.

AUTHOR INFORMATION

Corresponding Author

*Tel: +001 206-616-6509. Fax: +001 206-685-3451. E-mail: sjiang@uw.edu.

ORCID

Shaoyi Jiang: 0000-0001-9863-6899

Notes

The authors declare no competing financial interest.

ACKNOWLEDGMENTS

This work was supported by the National Science Foundation (DMR 1708436 and DMR 1307375), the Defense Advanced Research Projects Agency (N66001-12-1-4263), and the Office of Naval Research (N00014-14-1-0099 and N00014-15-1-2277).

REFERENCES

(1) Park, J.; Nam, J.; Won, N.; Jin, H.; Jung, S.; Cho, S. H.; Kim, S. Compact and Stable Quantum Dots with Positive, Negative, or Zwitterionic Surface: Specific Cell Interactions and Non-Specific Adsorptions by the Surface Charges. *Adv. Funct. Mater.* **2011**, *21* (9), 1558−1566.

(2) Alivisatos, P. The Use of Nanocrystals in Biological Detection. *Nat. Biotechnol.* **2004**, *22* (1), 47−52.

(3) Alivisatos, A. P. Semiconductor Clusters, Nanocrystals, and Quantum Dots. *Science* **1996**, *271* (5251), 933−937.

(4) Susumu, K.; Uyeda, H. T.; Medintz, I. L.; Pons, T.; Delehanty, J. B.; Mattoussi, H. Enhancing the Stability and Biological Functionalities of Quantum Dots via Compact Multifunctional Ligands. *J. Am. Chem. Soc.* **2007**, *129* (45), 13987−13996.

(5) Zrazhevskiy, P.; Sena, M.; Gao, X. H. Designing Multifunctional Quantum Dots for Bioimaging, Detection, and Drug Delivery. *Chem. Soc. Rev.* **2010**, *39* (11), 4326−4354.

(6) Chan, W. C. W.; Maxwell, D. J.; Gao, X. H.; Bailey, R. E.; Han, M. Y.; Nie, S. M. Luminescent Quantum Dots for Multiplexed Biological Detection and Imaging. *Curr. Opin. Biotechnol.* **2002**, *13*, 40−46.

(7) Liu, W.; Howarth, M.; Greytak, A. B.; Zheng, Y.; Nocera, D. G.; Ting, A. Y.; Bawendi, M. G. Compact Biocompatible Quantum Dots Functionalized for Cellular Imaging. *J. Am. Chem. Soc.* **2008**, *130* (4), 1274−1284.

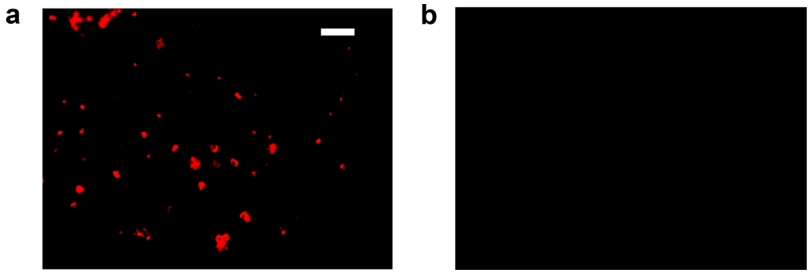

Figure 5. SA-functionalized CBSS-QDs bind specifically to biotin-labeled silicon particles (a) but do not bind SA-labeled silicone particles (b). Magnification 100× and scale bar 50 μm.

DOI: 10.1021/acs.langmuir.7b00981
Langmuir 2017, 33, 8784−8789

(8) Alivisatos, A. P.; Gu, W. W.; Larabell, C. Quantum dots as cellular probes. *Annu. Rev. Biomed. Eng.* **2005**, *7*, 55−76.
(9) Gao, X. H.; Yang, L. L.; Petros, J. A.; Marshal, F. F.; Simons, J. W.; Nie, S. M. In Vivo Molecular and Cellular Imaging with Quantum Dots. *Curr. Opin. Biotechnol.* **2005**, *16* (1), 63−72.
(10) Bentzen, E. L.; House, F.; Utley, T. J.; Crowe, J. E.; Wright, D. W. Progression of Respiratory Syncytial Virus Infection Monitored by Fluorescent Quantum Dot Probes. *Nano Lett.* **2005**, *5* (4), 591−595.
(11) Ballou, B.; Lagerholm, B. C.; Ernst, L. A.; Bruchez, M. P.; Waggoner, A. S. Noninvasive Imaging of Quantum Dots in Mice. *Bioconjugate Chem.* **2004**, *15* (1), 79−86.
(12) Daou, T. J.; Li, L.; Reiss, P.; Josserand, V.; Texier, I. Effect of Poly(ethylene glycol) Length on the in Vivo Behavior of Coated Quantum Dots. *Langmuir* **2009**, *25* (5), 3040−3044.
(13) Medintz, I. L.; Uyeda, H. T.; Goldman, E. R.; Mattoussi, H. Quantum Dot Bioconjugates for Imaging, Labelling and Sensing. *Nat. Mater.* **2005**, *4* (6), 435−446.
(14) Muro, E.; Pons, T.; Lequeux, N.; Fragola, A.; Sanson, N.; Lenkei, Z.; Dubertret, B. Small and Stable Sulfobetaine Zwitterionic Quantum Dots for Functional Live-Cell Imaging. *J. Am. Chem. Soc.* **2010**, *132* (13), 4556−4557.
(15) Wang, W. T.; Kapur, A.; Ji, X.; Zeng, B. R.; Mishra, D.; Mattoussi, H. Multifunctional and High Affinity Polymer Ligand that Provides Bio-Orthogonal Coating of Quantum Dots. *Bioconjugate Chem.* **2016**, *27*, 2024−2036.
(16) Giovanelli, E.; Muro, E.; Sitbon, G.; Hanafi, M.; Pons, T.; Dubertret, B.; Lequeux, N. Highly Enhanced Affinity of Multidentate versus Bidentate Zwitterionic Ligands for Long-Term Quantum Dot Bioimaging. *Langmuir* **2012**, *28*, 15177−15184.
(17) Zhan, N. Q.; Palui, G.; Safi, M.; Ji, X.; Mattoussi, H. Multidentate Zwitterionic Ligands Provide Compact and Highly Biocompatible Quantum Dots. *J. Am. Chem. Soc.* **2013**, *135*, 13786−13795.
(18) Tasso, M.; Giovanelli, E.; Zala, D.; Bouccara, S.; Fragola, A.; Hanafi, M.; Lenkei, Z.; Pons, T.; Lequeux, N. Sulfobetaine Vinylimidazole Block Copolymers: A Robust Quantum Dot Surface Chemistry Expanding Bioimaging's Horizons. *ACS Nano* **2015**, *9* (11), 11479−11489.
(19) Han, H. S.; Martin, J. D.; Lee, J.; Harris, D. K.; Fukumura, D.; Jain, R. K.; Bawendi, M. Spatial Charge Configuration Regulates Nanoparticle Transport and Binding Behavior In Vivo. *Angew. Chem., Int. Ed.* **2013**, *52*, 1414−1419.
(20) Ohyanagi, T.; Nagahori, N.; Shimawaki, K.; Hinou, H.; Yamashita, T.; Sasaki, A.; Jin, T.; Iwanaga, T.; Kinjo, M.; Nishimura, S. I. Importance of Sialic Acid Residues Illuminated by Live Animal Imaging Using Phosphorylcholine Self-Assembled Monolayer-Coated Quantum Dots. *J. Am. Chem. Soc.* **2011**, *133* (32), 12507−12517.
(21) Michalet, X.; Pinaud, F. F.; Bentolila, L. A.; Tsay, J. M.; Doose, S.; Li, J. J.; Sundaresan, G.; Wu, A. M.; Gambhir, S. S.; Weiss, S. Quantum Dots for Live Cells, in Vivo Imaging, and Diagnostics. *Science* **2005**, *307* (5709), 538−544.
(22) Lange, S. C.; van Andel, E.; Smulders, M. M. J.; Zuilhof, H. Efficient and Tunable Three-Dimensional Functionalization of Fully Zwitterionic Antifouling Surface Coatings. *Langmuir* **2016**, *32* (40), 10199−10205.
(23) Mattoussi, H.; Mauro, J. M.; Goldman, E. R.; Anderson, G. P.; Sundar, V. C.; Mikulec, F. V.; Bawendi, M. G. Self-Assembly of CdSe-ZnS Quantum Dot Bioconjugates Using an Engineered Recombinant Protein. *J. Am. Chem. Soc.* **2000**, *122* (49), 12142−12150.
(24) Zhang, L.; Xue, H.; Gao, C. L.; Carr, L.; Wang, J. N.; Chu, B. C.; Jiang, S. Y. Imaging and Cell Targeting Characteristics of Magnetic Nanoparticles Modified by a Functionalizable Zwitterionic Polymer with Adhesive 3,4-Dihydroxyphenyl-L-alanine Linkages. *Biomaterials* **2010**, *31* (25), 6582−6588.
(25) Yang, W.; Liu, S. S.; Bai, T.; Keefe, A. J.; Zhang, L.; Ella-Menye, J. R.; Li, Y. T.; Jiang, S. Y. Poly(carboxybetaine) Nanomaterials Enable Long Circulation and Prevent Polymer-Specific Antibody Production. *Nano Today* **2014**, *9*, 10−16.
(26) Smith, A. M.; Duan, H. W.; Rhyner, M. N.; Ruan, G.; Nie, S. M. A Systematic Examination of Surface Coatings on the Optical and Chemical Properties of Semiconductor Quantum Dots. *Phys. Chem. Chem. Phys.* **2006**, *8* (33), 3895−3903.
(27) Zhang, L. W.; Monteiro-Riviere, N. A. Mechanisms of Quantum Dot Nanoparticle Cellular Uptake. *Toxicol. Sci.* **2009**, *110* (1), 138−155.
(28) Barreto, J. A.; O'Malley, W.; Kubeil, M.; Graham, B.; Stephan, H.; Spiccia, L. Nanomaterials: Applications in Cancer Imaging and Therapy. *Adv. Mater.* **2011**, *23* (12), H18−H40.

DOI: 10.1021/acs.langmuir.7b00981
Langmuir 2017, 33, 8784−8789